Snail1 factor behaves as a therapeutic target in renal fibrosis

M. Teresa Grande[1,a], Cristina López-Blau[1], Berta Sánchez-Laorden[1], Cristina A. De Frutos[1,b], Agnès Boutet[1,c], R. Grant Rowe[2,d], Stephen J. Weiss[2], José M. López-Novoa[3] and M. Angela Nieto[1,*]

[1]Instituto de Neurociencias (CSIC-UMH), Avda. Ramón y Cajal s/n, 03550 San Juan de Alicante, Spain

[2] Division of Molecular Medicine and Genetics, Department of Internal Medicine, Life Sciences Institute, University of Michigan, Ann Arbor, MI 48109, USA

[3]Department of Physiology and Pharmacology, University of Salamanca, Campus Miguel de Unamuno, 37007 Salamanca, Spain.

Author for correspondence: M. Angela Nieto
e-mail: anieto@umh.es
Tel: 34-965919243

Present addresses:

[a]

[b] Ecole Normale Supérieure, Institut de Biologie de l'ENS (IBENS), Paris F-75005 France

[c] Station Biologique de Roscoff, CNTS-UPMC, UMR8227, Roscoff, France

[d]

Kidney fibrosis is a devastating disease that leads to organ failure, and no specific treatment is available to preserve organ function. In fibrosis, myofibroblasts accumulate in the interstitium leading to massive deposition of extracellular matrix and organ disfunction. The origin of myofibroblasts is multiple and the contribution of renal epithelial cells after undergoing epithelial-to-mesenchymal transition (EMT) is still debated. In a model unable to reactivate the EMT inducer Snail1 upon damage, we show that Snail1 is required in renal epithelial cells for the development of fibrosis. Damage-mediated Snail1 reactivation induces a partial EMT that relays fibrotic and inflammatory signals to the interstitium through the activation of TGF-β and NF-κB pathways. Snail1-induced fibrosis can be reverted in vivo and inhibiting Snail1 in a model of obstructive nephropathy highly ameliorates fibrosis. These results reconcile conflicting data on the role of EMT in renal fibrosis and provide avenues for the design of antifibrotic therapies.

Kidney fibrosis is the main cause leading to end-stage kidney failure in most progressive renal diseases[1] and the treatment of patients with end-stage renal disease cost only in the United States over $40 billion in 2009[2]. Importantly, the treatments are almost limited to some form of dialysis or to kidney transplant, as specific non-invasive alternatives are still missing. The development of the renal system involves several rounds of epithelial to mesenchymal and in particular, mesenchymal to epithelial transitions (EMT and MET, respectively[3]). Importantly, the suppression of this plasticity in the adult is fundamental to maintain tissue architecture and homeostasis. Snail1, a potent EMT inducer

both during embryonic development and tumor progression[4], is expressed in the precursors of the renal epithelial cells and it is downregulated upon epithelial differentiation and maintained silent in the adult[5]. We have previously shown that Snail1 reactivation in renal epithelial cells leads to renal fibrosis and renal failure in a tamoxifen-inducible Snail1 transgenic mouse model (Snail1-ERT2)[5]. Snail1 is also reactivated in mice subjected to unilateral ureteral obstruction (UUO)[6,7], a standard model for progressive renal fibrosis[8] and we found that Snail1 was highly reactivated in fibrotic lesions obtained from patients subjected to nephrectomy[5]. Together, these data indicate that Snail1 reactivation in adult kidneys is sufficient to induce renal fibrosis and that kidney fibrosis concurs with Snail1 activation in animal models and in patients. However, those observations do not address the question of whether Snail1 reactivation, and in turn, the activation of an EMT-like program is required for renal fibrosis to develop. While initial cell fate tracing experiments described a significant contribution of renal epithelial cells to myofibroblasts[9], subsequent studies could not find labeled epithelial cells within the interstitium[10,11]. Thus, we set out to directly assess whether the reactivation of Snail1 is not only sufficient but also required for the development of kidney fibrosis and whether its inhibition could have a significant impact on the disease. Using different mouse models we provide information on the mechanism behind Snail1 contribution to fibrosis. In addition, we show evidence of the activation of a partial EMT in epithelial cells that, without directly generating interstitial myofibroblats, relays crucial signals for the differentiation of this cell population and significantly impinges into the inflammatory response. This mechanism that, on one hand, leads to dedifferentiation of renal tubules while preserving its integrity and, on

the other hand facilitates interstitial fibrosis, also allows the regeneration of the damaged tubular epithelium. As such, we show that fibrosis can be reverted in vivo and that Snail1 inhibition significantly reverts renal fibrosis.

RESULTS

UUO-induced fibrosis is highly attenuated in kidneys that cannot reactivate Snail1 upon damage

To directly assess the contribution of Snail1 reactivation in epithelial cells to renal fibrosis, we crossed Snail1^{loxp} mice[12] with a strain bearing the *Ksp1.3-Cre* transgene[13]. Ksp cadherin is also known as Cadherin-16, a kidney-specific cadherin expressed in the cortex and the medulla. The resulting strain, *Ksp1.3-Cre*; Snail1$^{f/f}$, will be referred to as SFKC hereafter (**Supplementary Fig. 1**) and impedes Snail1 expression in Cadherin-16 positive cells. We chose this model because Snail1 expression is silent in the adult kidney but it is reactivated after UUO both in the cortex and in the medulla (**Supplementary Fig. 1**). During renal development, the onset of expression of Cadherin-16 coincides with that of Snail1 downregulation. In fact, Snail1 is a strong *Cadherin-16* repressor[4], and it is only when Snail1 is downregulated that renal cells express Cadherin-16 and epithelialization occurs. Therefore, preventing Snail1 expression in Cadherin-16 positive cells in the healthy adult kidney does not have any impact and the kidneys of these mice are completely normal. However, in contrast to the situation in wild type kidneys and as expected from the design of the experiment, SFKC mice were unable to reactivate *Snail1* expression in renal epithelial cells in response to UUO (**Fig. 1a,b**). Analysis of overall morphology,

collagen deposition assessed by Sirius red staining and expression of alpha smooth muscle actin (α-SMA) and vimentin shows that kidneys from SFKC mice are protected from the development of overt fibrosis after UUO, although signs of tubular distension resulting from the obstruction are readily evident (**Fig. 1b**). Quantitative analysis of epithelial and mesenchymal markers confirm the previously observed changes as a response to injury in wild type kidneys, changes that are very much attenuated in those from SFKC mice (**Fig. 1c**), particularly 2 weeks after UUO. These data indicate that Snail1 activation in renal epithelial cells significantly contributes to renal fibrosis.

The decrease in epithelial markers, the increase in mesenchymal markers observed in wild type mice after UUO and the high attenuation of these features in SFKC mice is compatible with Snail1 reactivation in fibrosis acting as an EMT inducer. If a full EMT program were activated in renal epithelial cells to contribute to myofibroblast, the prediction would be that those transformed epithelial cells were found in the interstitium. However, previous studies[10,11] failed to find these cells and a recent comprehensive cell tracing analysis of different kidney cells found a contribution of epithelial cells to the α-SMA+ myofibroblast population that appears after UUO of only around 5%[14]. The latter is compatible with our findings in wild type obstructed kidneys where we observed a small population of epithelial-derived cells, as confirmed by residual lectin staining, that clearly showed a mesenchymal phenotype without showing signs of dying and that were not well integrated into tubules (**Fig. 2a and Supplementary Fig. 2a**). The small percentage of those mesenchymal cells is also in keeping with the observation that in our experiments the total number of tubules does not significantly differs between control and SFKC kidneys after

UUO, although the number of dilated tubules is significantly smaller in SFKC obstructed kidneys (**Fig. 2b**). All of this is indicative of a limited full EMT process during fibrotic response after ureteral obstruction. Nevertheless, UUO induces the loss of polarity/differentiation as seen by the disappearance of lectin expression in renal epithelial cells that have reactivated Snail1 (**Fig. 2c**). Epithelial cells also activate the expression of the *Collagen I* gene (**Fig. 2d**), which, as *Snail2,* is also downstream of Snail1 in the kidney[5]. This indicates that tubular epithelial cells can contribute to collagen deposition even if they are still integrated in the tubules and that UUO-induced Snail1 reactivation triggers a partial EMT in both cortical and medullar renal epithelial cells leading to damaged tubules and collecting ducts. As none of this occurs in the SFKC kidneys (**Supplementary Fig. 2c,d**), we conclude Snail1 reactivation in renal epithelial cells has a big impact on the development of fibrosis.

Snail1 reactivation in the damaged kidney contributes to TGF-β signaling and inflammation

Our previous results suggest that damaged Snail1-expressing renal epithelial cells not only can contribute to collagen deposition while being integrated in the tubules but also send signals to the interstitium. As such, injured epithelial cells produce TGF-β-containing exosomes that promote the proliferation and activation of interstitial fibroblasts[15]. TGF-β signaling is also important for the differentiation of myofibroblasts from bone marrow-derived mesenchymal stem cells[15]. In relation to this, we found that *Tgf-β* expression is dependent on Snail1 expression, as it is the activation of the TGF-β pathway in both epithelial and interstitial cells as measured by phospho-Smad2 staining

(**Fig.3 a, b**). Thus, the decrease in TGF-β signaling may explain the high decrease in the α-SMA+ population in obstructed kidneys from SFKC mice (**Fig. 1b**). As myofibroblasts are also involved in the recruitment of macrophages, we examined F4/80 expression and observed that the degree of macrophage colonization in SFKC kidneys was highly attenuated, as it also was the overall inflammatory response as indicated by the decreased levels of nuclear phospho-NF-kB (**Fig. 3c**). Taking advantage of the LacZ reporter allele in our SFKC mice, we found that phospho-NF-κB labeling was only present in tubules that had not recombined (X-gal negative tubules) and therefore, they were competent to reactivate Snail1 (**Fig. 3d**)**.** Altogether these data indicate that UUO□induced fibrosis concurs with a partial EMT of renal epithelial cells mediated by the reactivation of Snail1 which activates TGF-β and TGF-β pathways, impacting on interstitial fibroblast activation, macrophage recruitment and the inflammatory response, all required for the development and progression of organ fibrosis.

Snail1-induced fibrosis can be reverted in vivo

Considering the high degree of epithelial plasticity observed during embryonic development and cancer in terms of EMT and its reverse process MET[16], we wanted to examine whether some plasticity also exists in fibrotic tissues. As damaged renal epithelial cells are important for the development of fibrosis we chose to test this in the Snail1-ERT2 model that we generated previously[5]. These mice can activate Snail1 by nuclear translocation of the protein following tamoxifen administration, and the model is very appropriate to test potential

reversibility because these mice (i) develop renal fibrosis upon Snail1 activation[5] and importantly, (ii) it is renal epithelial cell-specific (**Supplementary Fig. 3**). Thus, we decided to test whether Snail1-induced fibrosis could be reverted upon Snail1 downregulation. First, using the same model of inducible Snail1 reactivation, we examined whether Snail1-induced EMT can be reverted upon tamoxifen removal in kidney cells in culture. MDCK-Snail1-ERT2 cells treated with tamoxifen translocated Snail1 protein to the nucleus and undergone EMT. This transition was reverted after tamoxifen removal, concomitant with the absence of nuclear Snail1 and the recovery of epithelial morphology (**Supplementary Fig. 4**).

Next, we tested whether Snail1-induced fibrosis could be attenuated in vivo (**Fig. 4a**). As we had observed in kidney cells in culture, Snail1 protein can efficiently shuttle from the cytoplasm to the nucleus upon tamoxifen administration and it is detected back in the cytoplasm after tamoxifen removal (**Fig. 4b**). Fibrosis progresses with the time of tamoxifen exposure (8 versus 16 weeks, panels 2 and 3, respectively, in Fig. 4b) as seen by histology, Sirius red staining and changes in the expression of mesenchymal and epithelial markers detected either by immunostaining or gene expression analyses. Fibrosis also progresses with the activation of *Tgf-β* gene expression and an increase in the inflammatory response (nuclear pNF-κB) (**Fig. 4b,c**). All these features are highly attenuated after 8 weeks of tamoxifen removal. Particularly, collagen deposition, mesenchymal markers, *Tgf-β* expression and inflammation almost return to basal levels (**Fig. 4b,c**, compare panels 4 with 1 and real time RT-PCR data in the same groups). Furthermore, renal function assessed by the levels of creatinin clearance also shifted back to normal after being decreased upon 8 or

16 weeks of Snail1 reactivation. Altogether, these data indicate that Snail1 is a very potent inducer of fibrosis, and that this fibrosis can be reverted in vivo. However, this experimental design does not address whether renal fibrosis developed as a response to natural stimuli including damage could also be reverted after inhibiting Snail1.

Ureteral obstruction-induced fibrosis can be reverted by inhibiting Snail1

In order to examine whether inhibiting Snail1 could be beneficial in a more physiological context than the Snail1-ERT2 mice, we decided to inhibit Snail1 function in the UUO model. Seven days after UUO, when mice had already developed fibrosis, we injected VIVO-morpholinos designed against a splicing site in the *Snail1* mRNA (**Fig. 5a**; **Supplementary Fig. 6** and Methods), which allowed us to test the levels of the correctly spliced isoform and those in which exon 2 was missing. Therefore, we could assess the efficiency of the Morpholino in blocking Snail1 expression in each individual mouse, and compare this with the progression of fibrosis (**Supplementary Figure 6**). When we compared mice subjected to UUO for 7 days and then treated with either control morpholino (Control-MO) or one designed against *Snail1* mRNA (Snail1-MO), we observed a significant amelioration in fibrosis only in the Snail1-MO injected mice. Kidneys presented a recovered morphology a decrease in collagen deposition, and in vimentin and α-SMA expression in Snail1-MO treated mice (**Fig. 5b**). Similarly, expression analysis of transcripts indicated that the levels of *Snail1*, *Snail2* and *vimentin* were significantly downregulated when compared with those in obstructed kidneys from mice injected with

Control-MO (**Fig. 5c**). Furthermore, as suggested in our analyses of the SFKC mice, Snail1 had a big impact in TGF-β expression and macrophage colonization and inflammation (**Fig. 5b,c**), as all these responses were highly attenuated upon Snail1 inhibition. These results indicate that the amelioration in fibrosis observed in our mice is specific for Snail1 downregulation as it does not occur after Control-MO injection or even after the injection of Snail1-MO in mice in which the morpholino did not efficiently blocked normal mRNA splicing (**Supplementary Fig. 6**). In summary, this data indicate that Snail1 inhibition can significantly attenuate UUO-induced fibrosis in mice.

DISCUSSION

Renal fibrosis and organ failure is the end-stage of multiple chronic kidney diseases (CKD) that can result from urinary obstruction, autoimmune disorders, unresolved inflammation or deterioration of transplants[1]. In spite of the efforts invested no specific therapy is still available and the intimate mechanisms that drive interstitial fibrosis are still under debate, as conflicting results have either assigned an important or a negligible role of tubular EMT in the progression of renal fibrosis[9-11,17,18]. In addition, inflammatory cytokines and inflammatory cells are the principal effectors of the chronic disease[19], but the mechanisms by which chronic inflammation impinges into fibrogenesis still remain unclear. Understanding this link is envisaged as key in the design of therapeutic strategies to halt the progression of CKD[20]. Using renal epithelial-specific mouse models, and in particular modifying Snail1 expression in medullar and cortical renal epithelial cells, we have provided evidence of the contribution of EMT and the link between inflammation and fibrosis.

With respect to the EMT, we show that (i) a partial EMT of renal epithelial cells is activated upon renal damage, (ii) these damaged cells mainly remain integrated in the tubules while relaying fibrogenic and inflammatory signals that lead to the progression of the disease, and (iii) both fibrogenesis and inflammation require the activation and maintenance of the potent EMT inducer Snail1. Therefore, our results highlight the importance of an EMT-like program in renal epithelial cells for the development of fibrosis. They also reconcile previous conflicting results on the role of EMT[9-11] in this process, confirming the limited contribution of a full EMT program that delivers transformed epithelial cells to the interstitium[14]. Importantly, the partial EMT undergone by renal epithelial cells and the persistence of the damaged tubules explains the high degree of cell plasticity that we observed in vivo, as we show that Snail1 inactivation in a Snail1-induced fibrosis model leads to the recovery of renal morphology and function. In relation to this, during TGF-β-induced EMT in cancer cells, the mutual antagonism between Snail1 and miR-34, has been recently considered as a reversible switch, pointing to the possibility of reversion to the epithelial phenotype[21] and miR-34c has been shown to attenuate UUO-induced fibrosis[22]. Furthermore, our data help to better distinguish type2 EMT, previously ascribed to fibrosis and wound healing, from type3 EMT[23], associated with cancer cell delamination from the primary tumor. In the partial EMT that occurs in type2, damaged adult epithelial cells remain confined in their tissue of origin, while a full EMT in cancer (type3) endows cells not only with the ability to invade adjacent territories but also with that of intravasating into blood vessels to disseminate and later populate distant organs[16].

With regard to the link between fibrosis and inflammation we find that it also relies on the reactivation and, particularly, on the maintenance of Snail1 expression in epithelial cells. UUO induces the activation of TGF-β and NF-κB signaling pathways, key for fibrogenesis and inflammation, respectively, and the main drivers of CKD and other fibrotic processes[24,25]. The initial inflammatory response after UUO leads to TNF-α production, which induces the activation of NF-κB (reviewed in ref. 25). In addition to inflammation, NF-κB also impinges into Snail1 expression by directly inducing its transcription and the stabilization of the Snail1 protein[26]. TGF-β is first secreted to control the inflammatory response, but in the context of chronic injury as in fibrosis, it becomes fibrogenic and the most potent Snail inducer[4]. Thus, both signaling pathways converge in Snail1 and we find Snail1 activation and maintenance is required for the progression of fibrogenesis and for sustained inflammation. This indicates that Snail1 may establish positive feedback loops reinforcing both the fibrogenic and inflammatory responses. As such, we show that Snail1 is required for the maintenance of *Tgf-β* expression and in a context of activated NF-κB, Snail1 can mediate the induction of inflammatory cytokines, as observed in cancer cells[27]. Altogether, this explains why in the absence of Snail1, as in our SFKC model, both fibrogenesis and inflammation are highly attenuated, indicating that the partial EMT activated by Snail1 in renal epithelial cells is instrumental for the progression of renal disease.

Following the previous observations, Snail1 should behave as a promising therapeutic target. As such, we find that after UUO Snail1 inhibition by systemic injection of antisense oligonucleotides very significantly ameliorates fibrosis. Inhibiting EMT/inflammation by dowregulation of either TGF-β[28,29] or

NF-κB[30,31] signaling pathways have provided hope for antifibrotic treatments, but the pleiotropic roles of both pathways, particularly the associated beneficial effects, limit the potential use of their inhibitors in systemic administration protocols[32,33]. Given that Snail1 is maintained almost silent in healthy adult tissues[16], its inhibition should not cause undesirable side effects. Our data also provide a window of opportunity for the EMT inhibitors that are being developed for anti-metastatic therapies and that have been recently challenged by the demonstration that cancer cells need to revert to the epithelial phenotype for successful metastatic colonization[34,35]. As such, inhibiting EMT in cancer patients may be counterproductive. By contrast, the mesenchymal phenotype is the end stage in organ fibrosis and the reversion to the epithelial state should be fully beneficial. Therefore, we propose that Snail1 is located at the center of a "core" pathway in fibrosis, defining "core" as a pathway which targeting is sufficient to limit the progression of the disease[32]. In summary, inhibiting EMT and Snail1 in particular can be regarded as a safe strategy to ameliorate fibrosis, especially in fibrotic processes where inflammation plays an important role in the progression of the disease.

References

1. Liu, Y. Cellular and molecular mechanisms of renal fibrosis. *Nature reviews. Nephrology* **7**, 684-696 (2011).
2. National Kidney and Urologic Diseases Information Clearing House. Kidney Disease Statistics for the United States. No 12-3895 (2012).
3. Dressler, G. Tubulogenesis in the developing mammalian kidney. *Trends in cell biology* **12**, 390-395 (2002).

4. Thiery, J.P., Acloque, H., Huang, R.Y. & Nieto, M.A. Epithelial-mesenchymal transitions in development and disease. *Cell* **139**, 871-890 (2009).

5. Boutet, A.*, et al.* Snail activation disrupts tissue homeostasis and induces fibrosis in the adult kidney. *The EMBO journal* **25**, 5603-5613 (2006).

6. Sato, M., Muragaki, Y., Saika, S., Roberts, A.B. & Ooshima, A. Targeted disruption of TGF-beta1/Smad3 signaling protects against renal tubulointerstitial fibrosis induced by unilateral ureteral obstruction. *The Journal of clinical investigation* **112**, 1486-1494 (2003).

7. Lange-Sperandio, B.*, et al.* Leukocytes induce epithelial to mesenchymal transition after unilateral ureteral obstruction in neonatal mice. *The American journal of pathology* **171**, 861-871 (2007).

8. Chevalier, R.L., Forbes, M.S. & Thornhill, B.A. Ureteral obstruction as a model of renal interstitial fibrosis and obstructive nephropathy. *Kidney international* **75**, 1145-1152 (2009).

9. Iwano, M.*, et al.* Evidence that fibroblasts derive from epithelium during tissue fibrosis. *The Journal of clinical investigation* **110**, 341-350 (2002).

10. Humphreys, B.D.*, et al.* Fate tracing reveals the pericyte and not epithelial origin of myofibroblasts in kidney fibrosis. *The American journal of pathology* **176**, 85-97 (2010).

11. Li, L., Zepeda-Orozco, D., Black, R. & Lin, F. Autophagy is a component of epithelial cell fate in obstructive uropathy. *The American journal of pathology* **176**, 1767-1778 (2010).

12. Rowe, R.G.*, et al.* Mesenchymal cells reactivate Snail1 expression to drive three-dimensional invasion programs. *The Journal of cell biology* **184**, 399-408 (2009).
13. Shao, X., Somlo, S. & Igarashi, P. Epithelial-specific Cre/lox recombination in the developing kidney and genitourinary tract. *Journal of the American Society of Nephrology : JASN* **13**, 1837-1846 (2002).
14. LeBleu, V.S.*, et al.* Origin and function of myofibroblasts in kidney fibrosis. *Nature medicine* **19**, 1047-1053 (2013).
15. Borges, F.T.*, et al.* TGF-beta1-containing exosomes from injured epithelial cells activate fibroblasts to initiate tissue regenerative responses and fibrosis. *Journal of the American Society of Nephrology : JASN* **24**, 385-392 (2013).
16. Nieto, M.A. Epithelial plasticity: a common theme in embryonic and cancer cells. *Science* **342**, 1234850 (2013).
17. Kriz, W., Kaissling, B. & Le Hir, M. Epithelial-mesenchymal transition (EMT) in kidney fibrosis: fact or fantasy? *The Journal of clinical investigation* **121**, 468-474 (2011).
18. Fragiadaki, M. & Mason, R.M. Epithelial-mesenchymal transition in renal fibrosis - evidence for and against. *International journal of experimental pathology* **92**, 143-150 (2011).
19. Zeisberg, M. & Neilson, E.G. Mechanisms of tubulointerstitial fibrosis. *Journal of the American Society of Nephrology : JASN* **21**, 1819-1834 (2010).
20. Meng, X.M., Nikolic-Paterson, D.J. & Lan, H.Y. Inflammatory processes in renal fibrosis. *Nature reviews. Nephrology* (2014).

21. Tian, X.J., Zhang, H. & Xing, J. Coupled reversible and irreversible bistable switches underlying TGFbeta-induced epithelial to mesenchymal transition. *Biophysical journal* **105**, 1079-1089 (2013).

22. Morizane, R.*, et al.* miR-34c attenuates epithelial-mesenchymal transition and kidney fibrosis with ureteral obstruction. *Scientific reports* **4**, 4578 (2014).

23. Kalluri, R. & Weinberg, R.A. The basics of epithelial-mesenchymal transition. *The Journal of clinical investigation* **119**, 1420-1428 (2009).

24. Liu, Y. Renal fibrosis: new insights into the pathogenesis and therapeutics. *Kidney international* **69**, 213-217 (2006).

25. Lopez-Novoa, J.M. & Nieto, M.A. Inflammation and EMT: an alliance towards organ fibrosis and cancer progression. *EMBO molecular medicine* **1**, 303-314 (2009).

26. Wu, Y.*, et al.* Stabilization of snail by NF-kappaB is required for inflammation-induced cell migration and invasion. *Cancer cell* **15**, 416-428 (2009).

27. Lyons, J.G.*, et al.* Snail up-regulates proinflammatory mediators and inhibits differentiation in oral keratinocytes. *Cancer research* **68**, 4525-4530 (2008).

28. Rosenbloom, J., Castro, S.V. & Jimenez, S.A. Narrative review: fibrotic diseases: cellular and molecular mechanisms and novel therapies. *Annals of internal medicine* **152**, 159-166 (2010).

29. Zeisberg, M.*, et al.* BMP-7 counteracts TGF-beta1-induced epithelial-to-mesenchymal transition and reverses chronic renal injury. *Nature medicine* **9**, 964-968 (2003).

30. Esteban, V.*, et al.* Angiotensin II, via AT1 and AT2 receptors and NF-kappaB pathway, regulates the inflammatory response in unilateral ureteral obstruction. *Journal of the American Society of Nephrology : JASN* **15**, 1514-1529 (2004).

31. Miyajima, A.*, et al.* Novel nuclear factor kappa B activation inhibitor prevents inflammatory injury in unilateral ureteral obstruction. *The Journal of urology* **169**, 1559-1563 (2003).

32. Mehal, W.Z., Iredale, J. & Friedman, S.L. Scraping fibrosis: expressway to the core of fibrosis. *Nature medicine* **17**, 552-553 (2011).

33. Luedde, T. & Schwabe, R.F. NF-kappaB in the liver--linking injury, fibrosis and hepatocellular carcinoma. *Nature reviews. Gastroenterology & hepatology* **8**, 108-118 (2011).

34. Tsai, J.H., Donaher, J.L., Murphy, D.A., Chau, S. & Yang, J. Spatiotemporal regulation of epithelial-mesenchymal transition is essential for squamous cell carcinoma metastasis. *Cancer cell* **22**, 725-736 (2012).

35. Ocana, O.H.*, et al.* Metastatic colonization requires the repression of the epithelial-mesenchymal transition inducer Prrx1. *Cancer cell* **22**, 709-724 (2012).

FIGURE LEGENDS

Figure 1. Snail reactivation is required for the development of UUO-induced fibrosis. (**a**) Scheme of the experimental approach. UUO was conducted in wild type (WT) or Ksp1.3-Cre;Snail1$^{fl/fl}$ (SFKC) mice, which were sacrificed 7 or 15 days after obstruction. (**b**) Kidney sections taken from sham-operated (control)

and obstructed kidneys (UUO) of WT and SFKC mice 7 days after surgery, were subjected to in situ hybridization for *Snai1* expression; hematoxilin-eosin (H/E) and Sirius red stainings, and alpha smooth muscle actin (α-SMA) or vimentin immunohistochemistry. Tissue sections are representative of 8 independent samples examined from each of 6-8 mice per group. (**c)** *Snail1, Snail2, E-cadherin, Cadherin-16* and *Vimentin* mRNA levels determined by qRT-PCR in obstructed (L) and in contralateral non-obstructed kidneys (NL) from both WT and SFKC mice 7 or 15 days after UUO. Data are normalized to sham-operated wild type levels and represent mean ± SEM for groups of 6–8 mice**.** ***p* < 0.01, ****p* < 0.001, *****p* < 0.0001, ns, non-significant.

Figure 2. Renal epithelial cells dedifferentiate after UUO. **(a)** Cell polarity is affected in the proximal and distal tubular epithelia after UUO. Double immunohistochemistry for LTA lectin (marker of proximal tubules; PT) and PNA lectin (marker of distal tubules; DT) and TUNEL staining identified cells undergoing apoptosis. Hematoxylin staining (HE) and TUNEL panels show the same sections taken from kidneys of 8-week old WT mice that were sham-operated (control) or subjected to obstruction (UUO), both sacrificed 7 days after the intervention. Damaged tubules downregulate lectin expression (see also Supplementary Fig. 2b). The fields are selected to illustrate lectin positive cells that are not integrated into the tubules, depict a mesenchymal phenotype and show internalized (non-polarized) lectin expression (stars). These cells represent a small percentage of renal epithelial cells (less than 5%) and they are TUNEL negative. (**b**) Number of dilated and total tubules in wild type (WT) and SFKC kidneys 15 days after UUO. 10 different fields were counted in 12

independent mice per condition. Data represent mean ± SEM. *$p < 0.05$; ns, non-significant. (**c**) Lectin staining (LTA), in sections from the same kidneys used in panel a, is downregulated in tubules that have reactivated Snail1 expression as shown by immunofluorescence. (**d**) *Collagen type I* gene expression (blue; stars) and LTA (brown) determined by in situ hybridization in kidneys from 8-week old wild type (WT) mice 7 days after UUO. *Collagen type I* gene is transcribed after UUO in wild type mice in epithelial and interstitial renal cells. Tissue sections are representative of 6 independent samples examined.

Figure 3. Snail1 reactivation in renal epithelial cells contributes to fibrosis by inducing TGF-β and an inflammatory response in the injured kidney. The experimental design is the same as in Fig. 1. (**a**) *Tgf*-β mRNA levels determined by qRT-PCR in obstructed (L) and contralateral control (NL) kidneys from wild type and SFKC mice 7 or 15 days after surgery. Data are normalized to sham-operated wild type levels and represent mean ± SEM for groups of 6–8 mice**.** ****$p < 0.0001$, ns, non-significant. (**b**) Phospho-Smad2 (p-Smad2) stainings in representative sections from sham-operated (control) and obstructed kidneys (UUO) from WT or SFKC mice collected 7 days after surgery (**c**) Immunolabeling for F4/80 (macrophage marker) and phospho-NF-κB (pNF-κB) in samples from the same experiment shown in panel b. (**d**) X-gal and pNF-κB staining in obstructed kidneys from SFKC mice. Tissue sections are representative of 6 independent samples examined per mouse (n=6).

Figure 4. Snail1-induced fibrosis can be reverted in vivo. (**a**) Scheme of the experimental approach. Mice were treated with (1) vehicle (corn oil, –TAM); (2)

tamoxifen for 8 weeks (+TAM); (3) tamoxifen for 16 weeks (+TAM+TAM), and (4) tamoxifen for 8 weeks followed by vehicle treatment for another 8 weeks (+TAM-TAM). Additional control experiments including treatment of wild type mice are shown in **Supplementary Fig. 5**. (**b**) Anti-human estrogen receptor (hER) staining showing exogenous Snail1 protein expressed in the cytoplasm of the transgenic kidneys (-TAM) and translocated to the nucleus upon tamoxifen administration (+TAM; +TAM+TAM). Snail1 is detected back in the cytoplasm after 8 weeks of tamoxifen removal (+TAM-TAM). Panels show hematoxilin-eosin (H/E) and Sirius red staining, and alpha smooth muscle actin (α-SMA), vimentin and phospho-NF-κB (pNF-κB) immunohistochemistry. Levels approach control levels upon tamoxifen removal. Tissue sections are representative of 6 independent samples examined. (**c**) mRNA levels detected by qRT-PCR in transgenic kidneys showing an increase in *Snail2*, *Vimentin* and *Tgf*-β mRNA levels and a decrease in *E-Cadherin* and *Cadherin-16* mRNA abundance upon Snail1 activation ((2;+TAM and 3;+TAM+TAM) and a return to levels close to the baseline after 8 weeks of tamoxifen removal (4:+TAM-TAM). Data are normalized to vehicle treated kidney levels (1; -TAM) and represent mean ± SEM for groups of 6–8 mice**.** *p< 0.05, ***p* < 0.01, ****p* < 0.001, *****p* < 0.0001, ns, non-significant.

Figure 5. Snail inactivation reverts UUO-induced fibrosis in mice. (**a**) Scheme of the experimental approach. Seven days after UUO, mice were injected with vivo-morpholino control (Control-MO) or Snail1-MO1 (Snail1-MO) every other day. (**b**) Hematoxilin-Eosin (H/E) and Sirius Red staining; expression of mesenchymal (vimentin and alpha smooth muscle actin (□-SMA)); and

inflammatory response markers (F4/80 and phospho-NFkB (pNFkB)) immnunohistochemistry in kidney sections from mice in panel a. Note the recovered morphology and epithelial markers expression together with decreased inflammation in obstructed kidneys injected with Snail1-MO. (**c**) qRT-PCR from obstructed kidneys treated with Snail1-MO shows a decrease in UUO-induced *Snail1* and *Snail2* mRNA levels, a highly diminished expression of the mesenchymal marker *vimentin* and of *Tgf-β*) plus a partial recovery of *E-Cadherin* and *Cadherin-16* transcripts. Data are normalized to contralateral non-obstructed kidney levels (NL) and represent mean ± SEM for triplicates of data from a representative mouse in which Snail1-MO efficiently induced exon-skipping and therefore, subsequent Snail1 downregulation**.** *p< 0.05, ***p* < 0.01, ***p* < 0.001, ****p* < 0.0001, ns, non-significant.

METHODS

Methods are included in Supplementary information

ACKNOWLEDGMENTS

We thank members of Angela Nieto's lab for helpful discussions and comments along the years. We are very grateful to Peter Igarashi (University of Texas Southwestern) for providing the Ksp1.3-Cre mice. This work was supported by grants from the Spanish Ministry of Economy and Competitivity (BFU2008-01042 and CONSOLIDER-INGENIO 2010 CSD2007-00023 and CDS2007-00017), the Generalitat Valenciana (Prometeo 2008/049 and PROMETEOII/2013/002) and the European Research Council (ERC AdG 322694) to M.A.N. The Instituto de Neurociencias is a Centre of Excellence Severo Ochoa. M.T.G. was recipient of a contract from the JAE-doc Program

(CSIC-European Social Fund).

AUTHOR CONTRIBUTIONS

M.T.G. performed the majority of experiments, analyzed the data and contributed to writing the manuscript, C.L.-B. helped in the surgery and histological and expression studies, B.S.-L. carried out statistical analyses and contributed to writing, C.A.F. and A.B. started the project, G.R. and S.J.W. provided the Snail1^{loxp} mice before publication, J.M.L.-N helped in the interpretation of data and M.A.N. conceived the project, interpreted the data and wrote the manuscript.

COMPETING FINANCIAL INTERESTS

The authors declare no competing financial interests

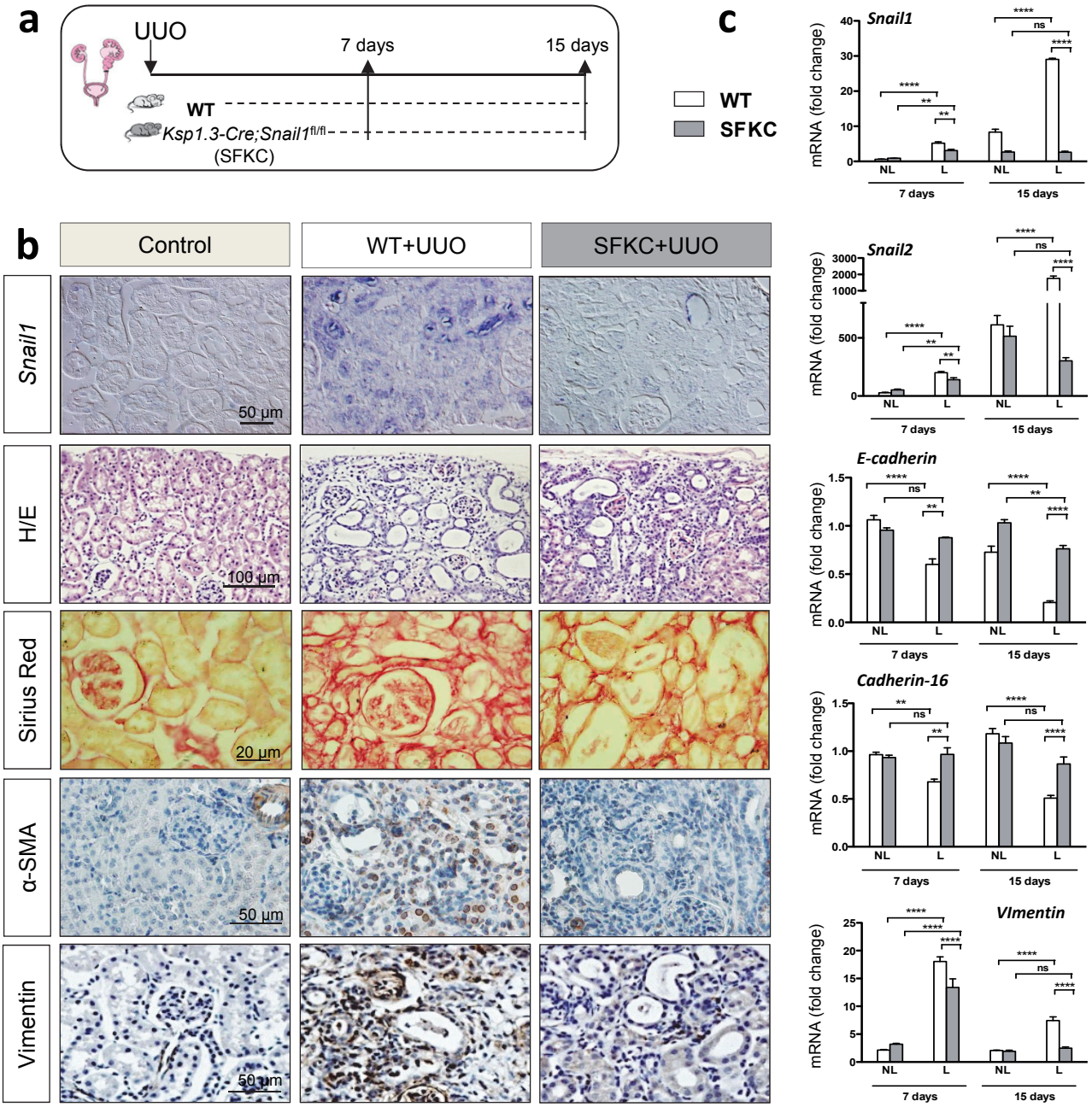
a
UUO
7 days
15 days
WT
Ksp1.3-Cre;Snail1fl/fl
(SFKC)
b
Control
WT+UUO
SFKC+UUO
Snail1
H/E
Sirius Red
α-SMA
Vimentin
50 μm
100 μm
20 μm
50 μm
50 μm
c
WT
SFKC
Snail1
Snail2
E-cadherin
Cadherin-16
Vimentin
mRNA (fold change)
NL
L
7 days
15 days

Figure 1

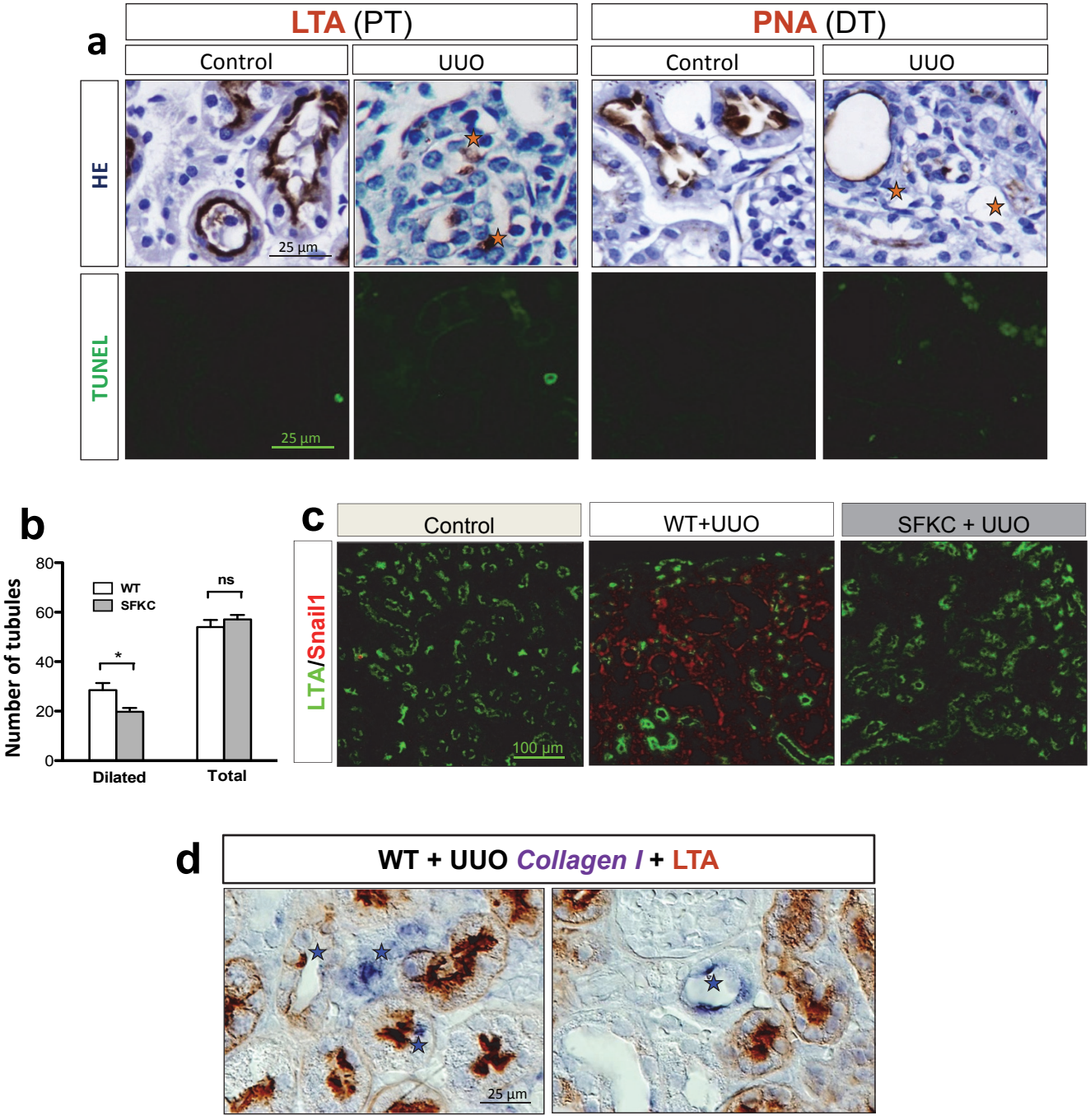
a
LTA (PT)
PNA (DT)
Control
UUO
Control
UUO
HE
TUNEL
25 µm
25 µm
b
Number of tubules
80
60
40
20
0
WT
SFKC
*
ns
Dilated
Total
c
Control
WT+UUO
SFKC + UUO
LTA/Snail1
100 µm
d
WT + UUO Collagen I + LTA
25 µm

Figure 2

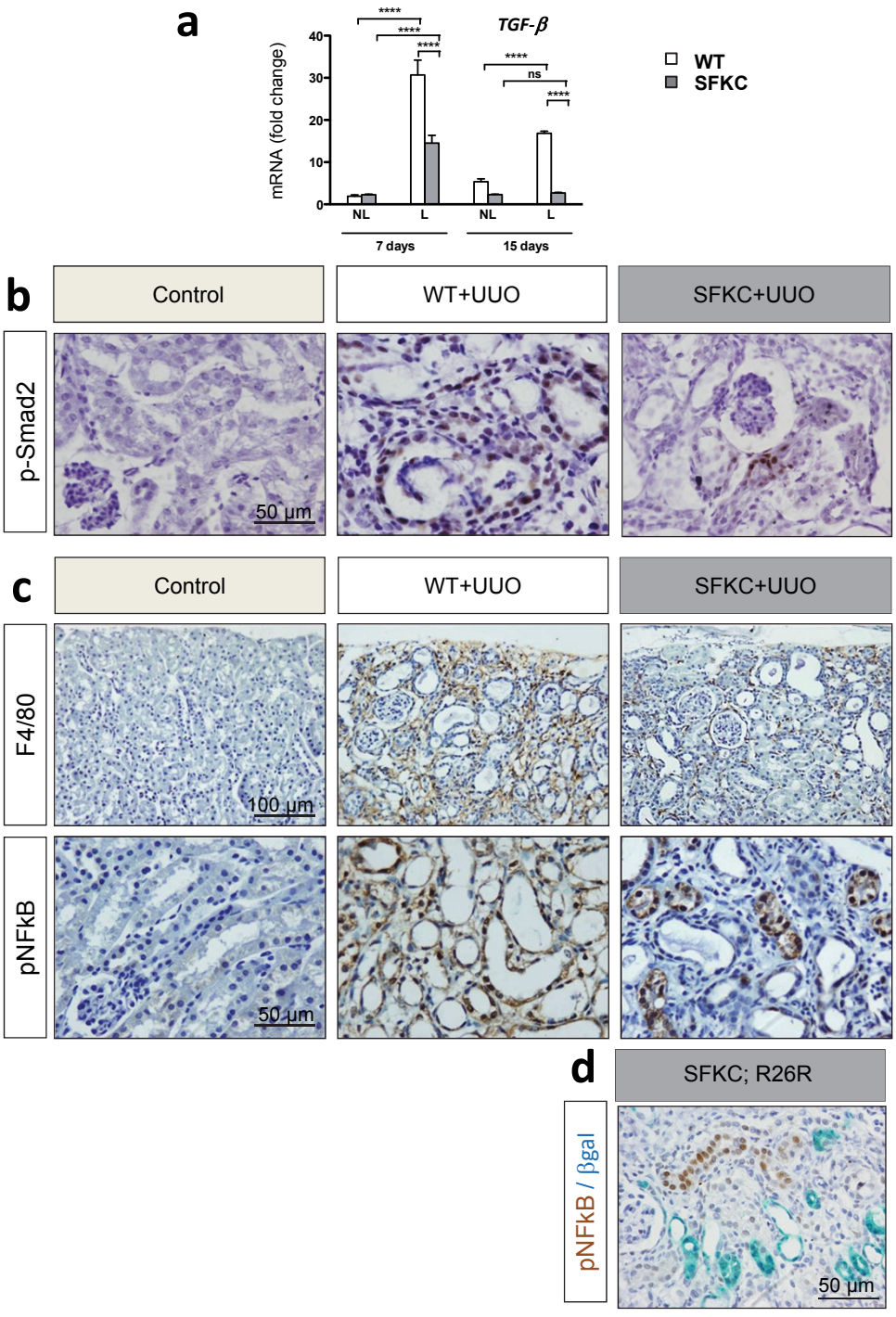
a
TGF-β
mRNA (fold change)
40
30
20
10
0
****
****
****
****
ns
****
NL
L
NL
L
7 days
15 days
WT
SFKC
b
Control
WT+UUO
SFKC+UUO
p-Smad2
50 μm
c
Control
WT+UUO
SFKC+UUO
F4/80
100 μm
pNFkB
50 μm
d
SFKC; R26R
pNFkB / βgal
50 μm

Figure 3

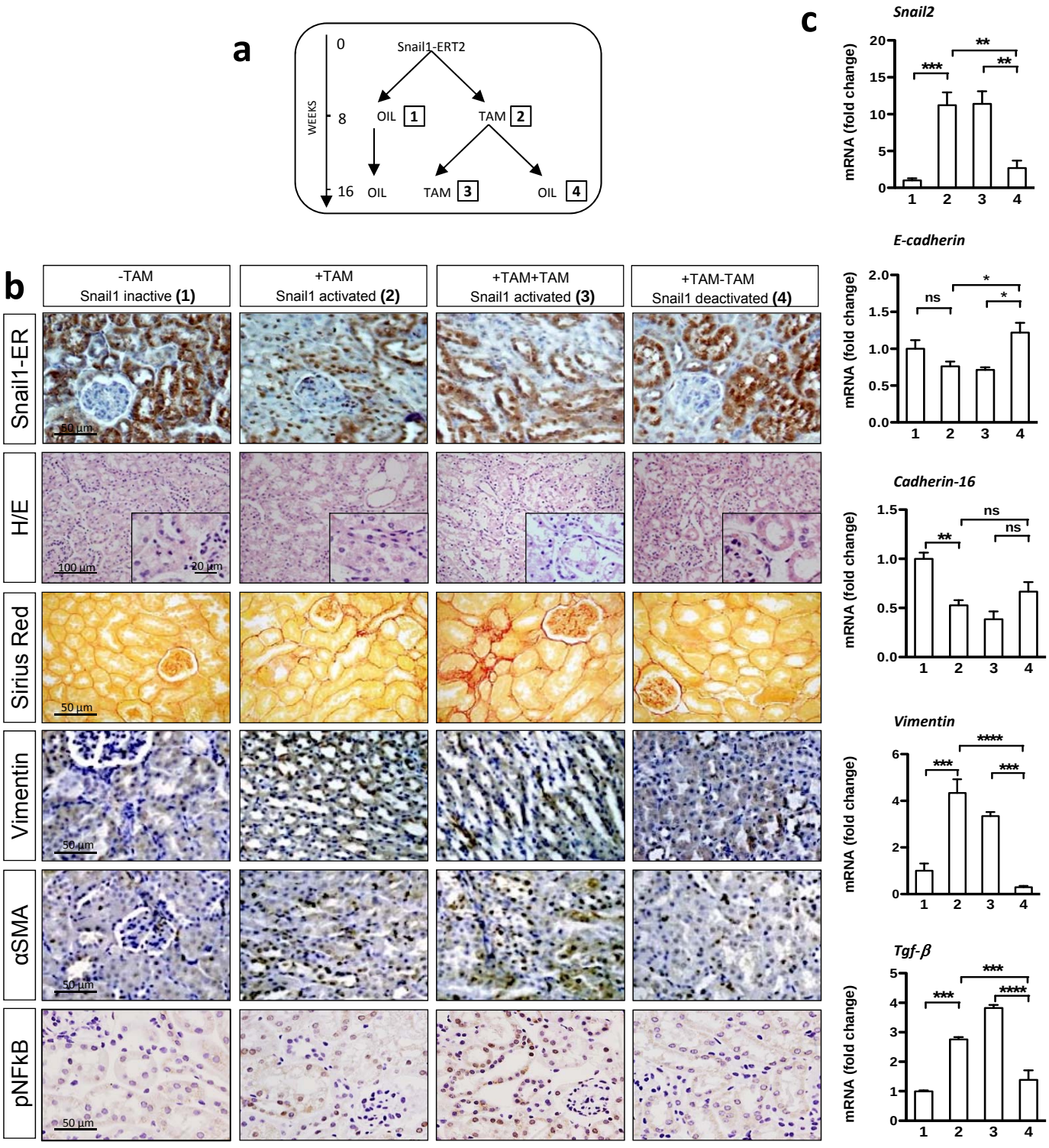
a
0
Snail1-ERT2
WEEKS
8
OIL 1
TAM 2
16
OIL
TAM 3
OIL 4
b
-TAM
Snail1 inactive (1)
+TAM
Snail1 activated (2)
+TAM+TAM
Snail1 activated (3)
+TAM-TAM
Snail1 deactivated (4)
Snail1-ER
H/E
Sirius Red
Vimentin
αSMA
pNFkB
50 µm
100 µm
20 µm
c
Snail2
E-cadherin
Cadherin-16
Vimentin
Tgf-β
mRNA (fold change)
ns

Figure 4

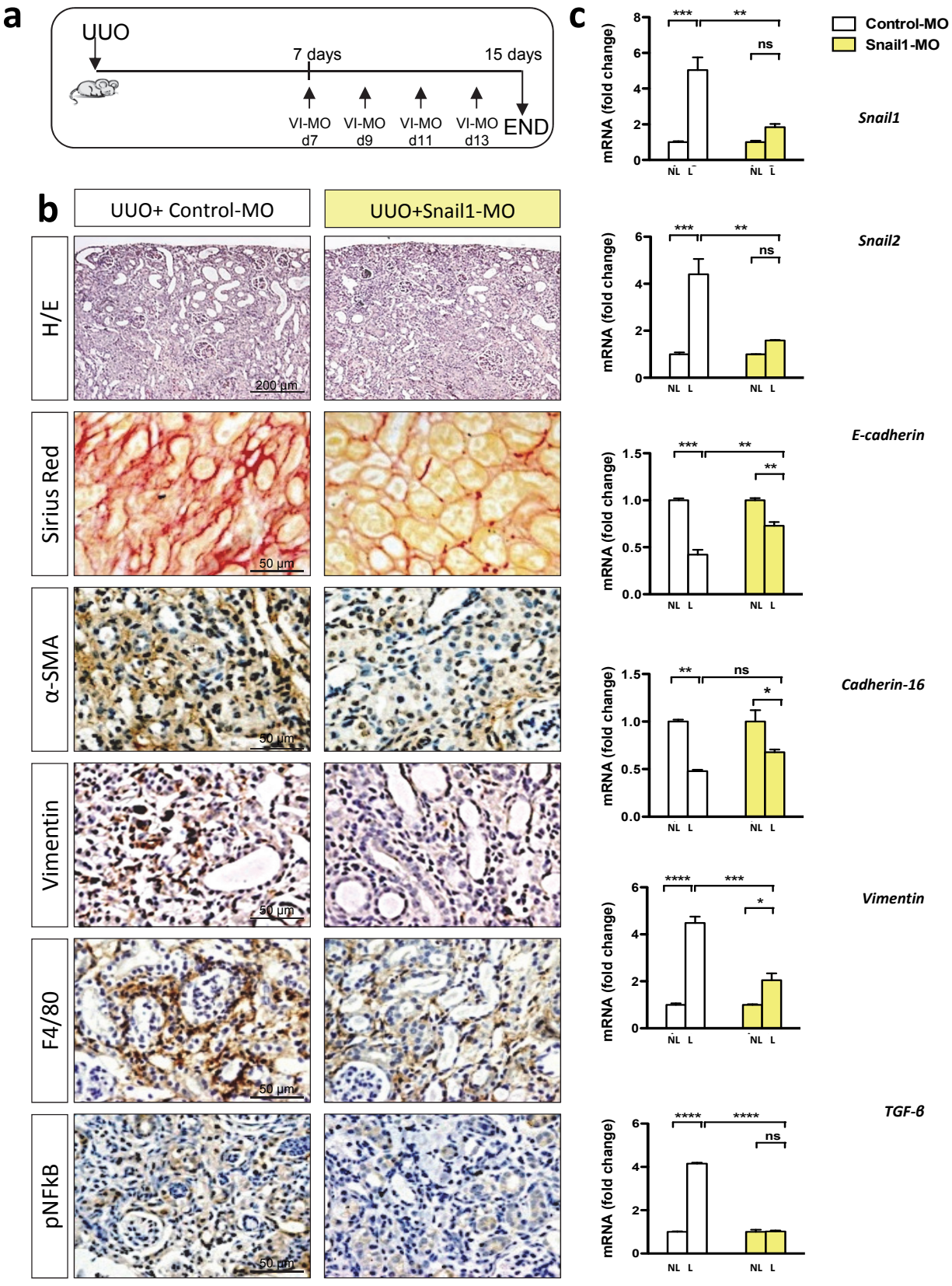
a
UUO
7 days
15 days
VI-MO d7
VI-MO d9
VI-MO d11
VI-MO d13
END
b
UUO+ Control-MO
UUO+Snail1-MO
H/E
Sirius Red
α-SMA
Vimentin
F4/80
pNFkB
200 μm
50 μm
c
Control-MO
Snail1-MO
mRNA (fold change)
NL L
Snail1
Snail2
E-cadherin
Cadherin-16
Vimentin
TGF-β
ns

Figure 5

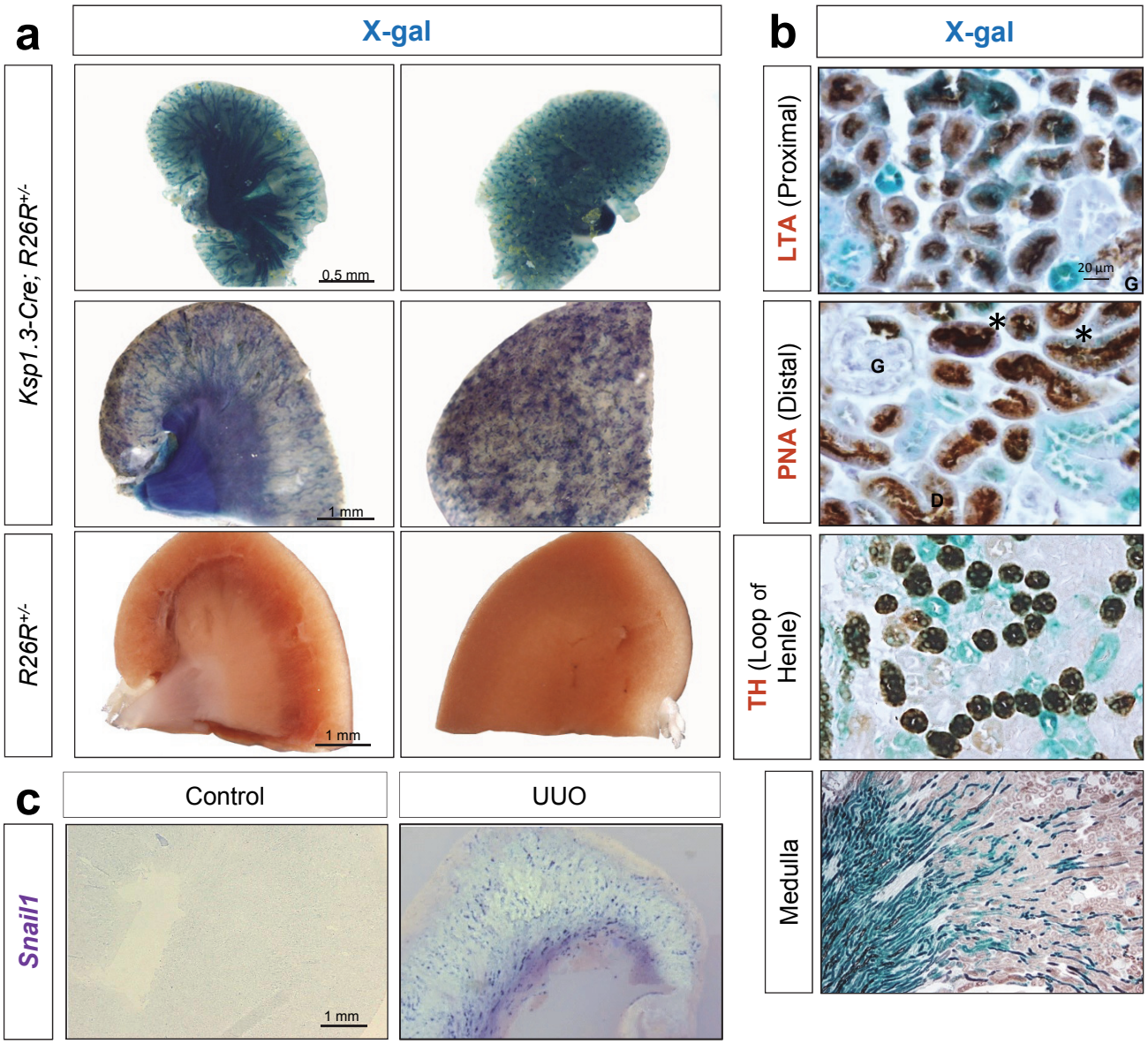

Supplementary Figure 1. Epithelial recombination mediated by *Ksp1.3-Cre* as assessed by crossing the mice with the Rosa26R (R26R) reporter strain. (**a**) Whole-mounted X-gal stained kidneys from *Ksp1.3Cre;R26R* newborn and adult mice (2-month-old) to detect β-galactosidase activity as an indication of Cre recombination. Recombination is detected in both kidney cortex and medulla. No staining is detected in kidneys from a transgenic mouse carrying only the *lacZ* reporter gene. (**b**) X-gal staining in sections obtained from *SFKC;R26R* kidneys and co-staining with different lectins, markers of proximal tubules (LTA) or distal tubules (PNA). Asterisks indicate examples of double positive tubules in the latter. Anti-Tam-Horsfall protein antibodies mark the thick ascending limb of Henle (TH). X-gal (β-galactosidase) staining is also prominent in the collecting ducts of the medulla. G indicates glomeruli. *Ksp1.3Cre* mediates recombination in collecting ducts, loop of Henle, the majority of proximal tubules and in some distal tubules. (**c**) *Snail1* expression is reactivated after UUO in both the cortex and the medulla. Control; sham-operated kidney.

Supplementary Figure 1

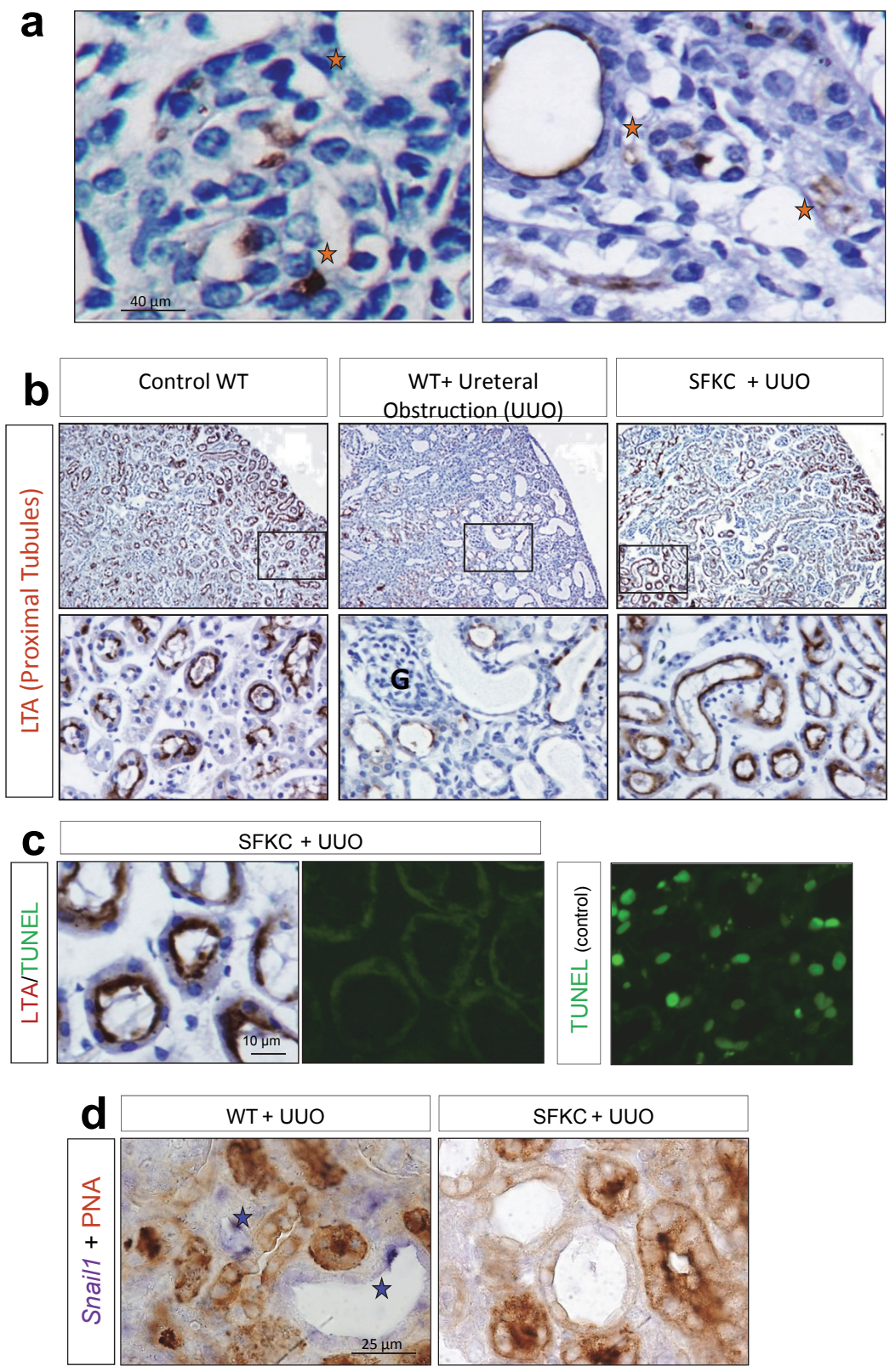

Supplementary Figure 2

Supplementary Figure 2. (**a**) High power magnification of two photomicrographs shown in Fig. 2a to better assess the position and morphology of mesenchymal cells. Stars indicate the position of these cells. (**b**) Low and high magnification images of sections taken from Sham-operated (control) and obstructed kidneys (UUO) from wild type and SFKC mice to better appreciate morphology together with lectin expression. Wild type kidneys undergo massive lectin loss although tubules are still present. SFKC kidneys maintain lectin expression and the number of dilated tubules is decreased. G indicates glomeruli. (**c**) No cell death is detected in SFKC kidney sections after seven days of UUO as assessed by TUNEL. (**d**) PNA (brown, detected by immunohistochemistry) and *Snail1* (blue, detected by in situ hybridization) expression is not induced in SFKC kidneys after UUO. Stars indicate *Snail1* expression.

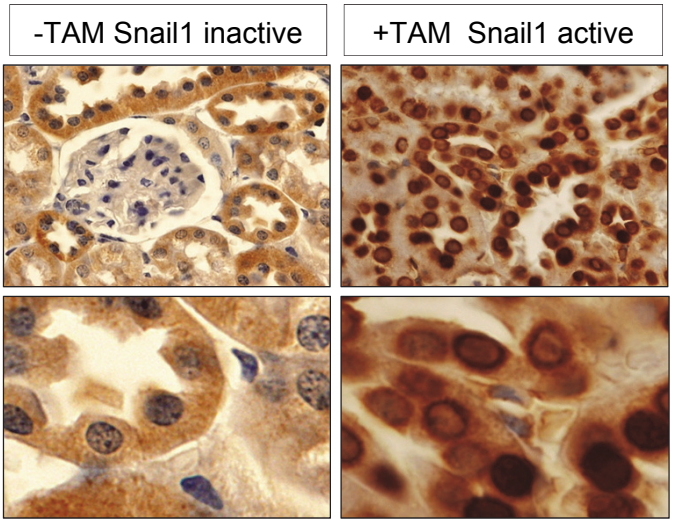

Supplementary Fig. 3. The Snail1-ERT mouse model is specific for renal epithelial cells. Transgenic Snail1 protein is translocated from the cytoplasm to the nucleus upon tamoxifen administration. Glomerular and endothelial cells do not express the transgenic protein.

Supplementary Figure 3

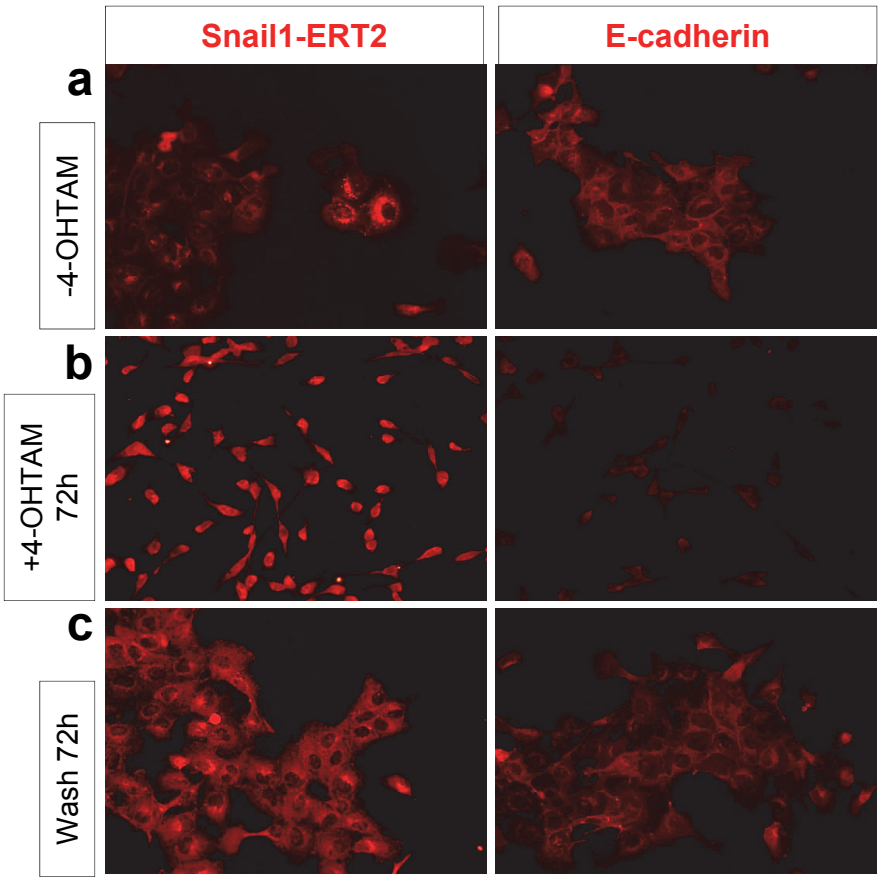

Supplementary Figure 4. (**a**) MDCK cells (dog renal cells) were transfected with the Snail1 tamoxifen inducible construct used to generate the Snail-ERT2 transgenic mouse line. (**b**) Cells were treated with 4-Hydroxytamoxifen (4'OH-TAM) for 72 hours and fixed for immunofluorescence analysis. Note that Snail1 is detected in the nucleus and cells have adopted a mesenchymal phenotype. (**c**) Cells were washed after 4'OH-TAM treatment and left in culture for an additional 72 hours period. Snail1 is absent from the nuclei and cells recover E-cadherin expression and lose mesenchymal morphology. 4'OH-TAM (200 ng/ml), the synthetic ligand recognized by the ligand-binding domain of the human estrogen receptor in our construct was used in this experiment. However, in vivo, tamoxifen (TAM) can be used as it is metabolized to 4'OH-TAM.

Supplementary Figure 4

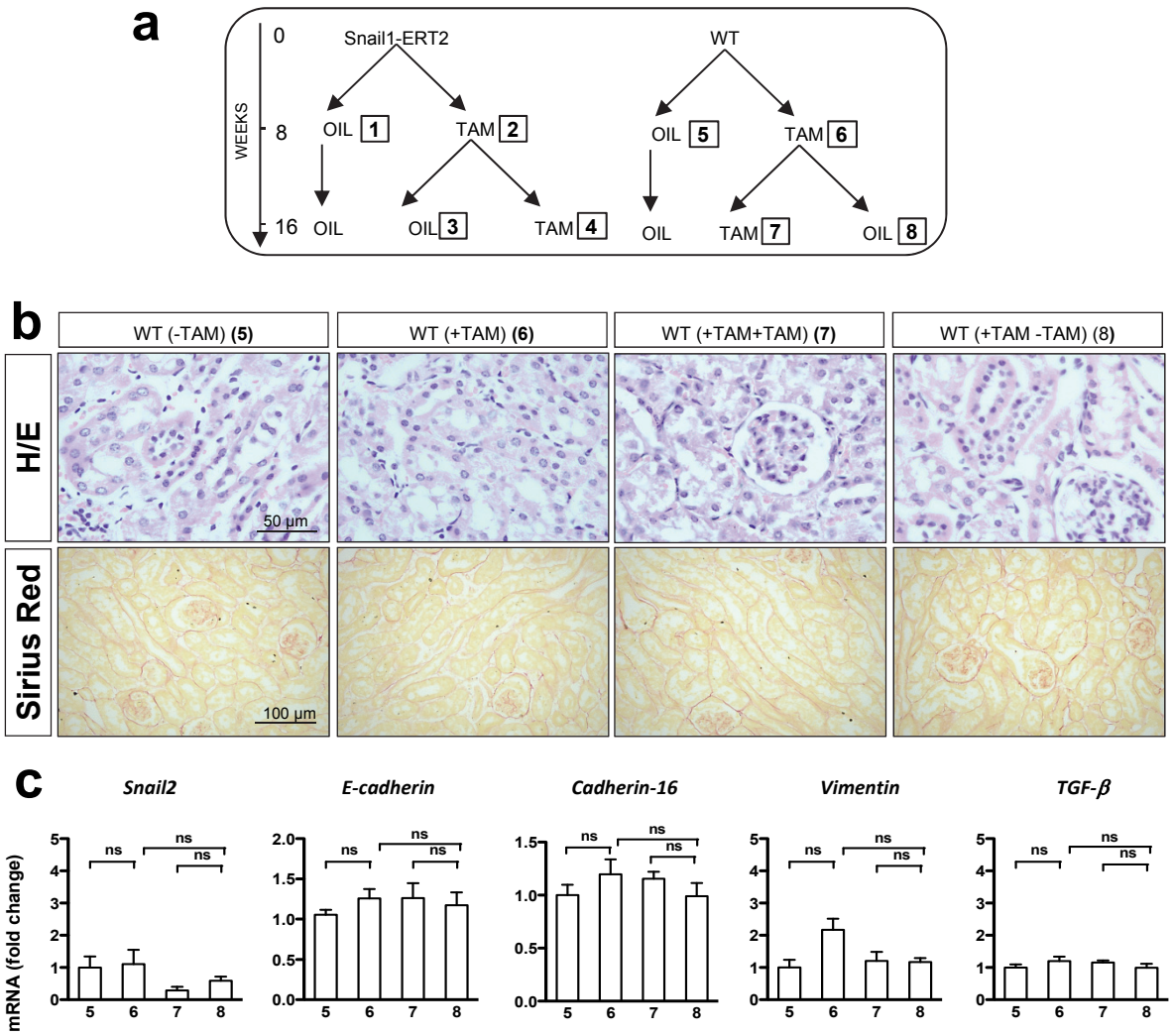

Supplementary Figure 5. (**a**) WT mice were treated with tamoxifen or corn oil (vehicle) in parallel to the treatments performed in Snail1-ERT2 mice shown in Fig. 4. (**b**) Stainings in 5 µm paraffin sections from wild type mice kidneys treated with corn oil (5), tamoxifen for 8 weeks or 16 weeks (6 or 7), or tamoxifen for 8 weeks followed by oil treatment for another 8 weeks (8). Hematoxilin-eosin (H/E) and Sirius red staining do not show any sign of fibrosis. Tissue sections are representative of 6 independent samples examined per mouse (n=4 per condition). **(c)** *Snail2*, *E-cadherin*, *Cadherin-16*, *vimentin* and *TGF-β* mRNA levels detected by qRT- PCR from WT kidneys does not detect any significant difference between treatments. Data are normalized to vehicle injected kidney levels (5) and represent the mean ± SEM of groups of 3-4 mice.

Supplementary Figure 5

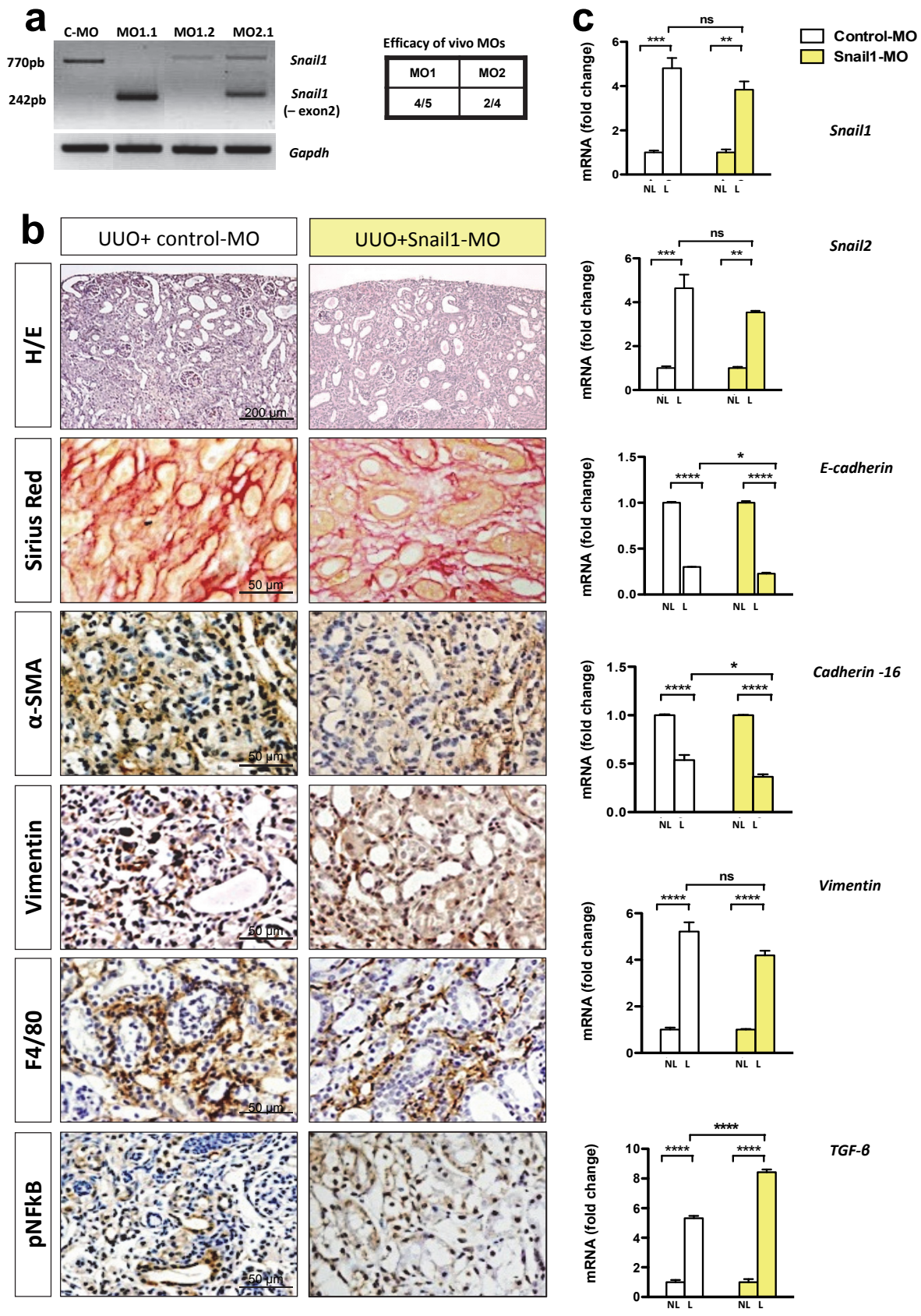

Supplementary Figure 6

Supplementary Figure 6. (**a**) RT-PCR analysis of *Snail1* transcripts expressed in obstructed kidneys after treatment with Vivo-morpholinos designed to induce exon skipping in *Snail1* mRNA. The full-length product amplified from the normal transcript is 770 base pairs (bp), and the product missing exon 2 is 242 bp. Two VIVO-morpholinos (MO) were designed as described in Online methods. MO1 efficiently induced exon skipping in 80% of injected mice (4/5), while MO2 only partly worked in 2/4 injected mice. (**b and c**) Panels show data from the mouse in which MO1 did not work as assessed by its failure in inducing exon skipping (MO1.2 in **a**). Samples were treated as those from the mice in which MO1 effectively led to exon skipping (4/5; example of one of these mice is MO1.1 in **a**, and the corresponding data are shown in Fig. 5). Hematoxilin-Eosin (H/E) and Sirius red staining, immunohistochemistry for mesenchymal markers (vimentin and alpha smooth muscle myosin; αSMA) and inflammation markers (F4/80 and phospho-NFkB (pNFkB) do not show significant differences between the mouse injected with MO1 or Control MO (panel **b**). qRT-PCR analysis fails to show significant differences in mRNA abundance except for *TGF-β*, which coincides with higher NFkB activation. We cannot discard that the injection of Snail1MO1 induced an inflammatory response that does not occur after injection of the control MO. This response is abolished when Snail MO1 efficiently induced exon skipping, further supporting the role of Snail1 in inflammation in the renal system. Data are normalized to contralateral non-obstructed kidneys (NL) and represent the mean ± SEM of triplicates (n = 5). $*p < 0.05$, $**p < 0.01$, $***p < 0.001$.

SUPPLEMENTARY INFORMATION

ONLINE METHODS

Mice. Animals were housed under SPF conditions at the RMG animal House (ES-119-002001 SEARMG). Work with GMO was under the A1ES/13/1-25 license. To specifically inactivate Snail1 in renal epithelial cells, we generated a mouse line with kidney-specific inactivation of Snail1 by crossing females from the snail-floxed line (*Snai1*$^{fl/fl}$)[1] with the Ksp-Cre transgenic strain obtained from Peter Igarashi´s lab[2]. R26R mice (Gtrosa26tm1Sor) were obtained from Jackson Laboratories. To examine the efficiency of recombination, heterozygous female Snail floxed mice (Snail1$^{fl/+}$) were crossed with heterozygous male mice that express Ksp1.3-Cre transgene. From the filial (F) 1 progeny, mice (male or female), litters with heterozygous deletion of *Snai1* gene that harboured the Ksp1.3/Cre transgene (*Snail1*$^{fl/+}$*; Ksp1.3-Cre*) were selected and they were further crossed with the opposite sex of Snail1 floxed mice (Snai1$^{fl/+}$) to obtain mice expressing complete deletion of Snail1 in the F2 progeny (Snai1$^{fl/fl}$;Ksp1.3-Cre), referred to as SFKC. Compared to control (*Snail1*$^{fl/fl}$) littermates, SFKC mice are viable, display no overt defects, and survive to 6 months and beyond with no ill effects. The generation of the tamoxifen-inducible Snail1 transgenic mouse has been described previously[3] where the transgenic Snail1-ERT2 protein was specifically expressed in renal epithelial cells (**Supplementary Fig. 3**). In this model, constitutively expressed exogenous Snail1 protein only becomes active on nuclear translocation. For tamoxifen inductions, the tamoxifen was dissolved in corn oil 30 mg/ml and mice (8 weeks-old) were intraperitoneally injected with 200 mg of tamoxifen per

gram of body weight or a similar volume of corn oil every 3 days for 8 or 16 weeks. Animals were killed by cervical dislocation and their kidneys processed for mRNA extraction, ISH or immunohistochemistry. All procedures were conducted in strict compliance with the European Community Council Directive (89/609/EEC) and the current Spanish legislation. Ethical protocols were approved by the CSIC Ethical Committee and the Animal Welfare Committee of the Instituto de Neurociencias.

UUO model. Mice (8 weeks-old) were anesthetized with an intraperitoneal injection of ketamine (100 mg/kg) and xylacine (10 mg/kg). The abdomen was opened, and the left ureter was ligated with 5-0 silk. The abdomen was then closed with running sutures and the skin was closed with interrupted sutures. After surgery, the mice were maintained in a temperature-controlled room with a 12 hours light/dark cycle, and were reared on standard chow and water ad libitum. Unilateral ureteral obstruction (UUO) was maintained for 7 or 15 days.

Renal function. Twenty-four-hour urine was collected from tamoxifen-inducible Snail1 transgenic mice, at baseline and after 8 or 16 weeks of tamoxifen or vehicle administration. Animals were housed in a metabolic cage for collection of urine to determine creatinine concentration and urine volume. Creatinine and acid uric was also measured in the blood obtained through the saphenous vein.

Morpholino oligomer and in vivo treatment. The oligonucleotides sequences 5′-TGAACTCTGCGGGAAGAGAAGAGAC-3′ VM1 against the boundary sequences of the intron 1 and exon 2 and 5´-

GCTATGCACACTCACTCACCAGTGT-3´ VM2 against the boundary sequences of the exon and intron 2 of Snail1 gene were synthesized as Morpholinos by (Gene Tools). Vivo-Morpholinos were made by conjugation of an unmodified Morpholino with a synthetic scaffold featuring eight guanidinium head groups. A control antisense that targets a human β-globin intron mutation 5′-CCTCTTACCTCATTACAATTTATA-3′ was used as vivo-morpholino standard control, VMC. C57/Bl6 mice aged 8 weeks were subjected to UUO and 7 days after obstruction they were injected every other day until day 15. A solution of containing vivo-Morpholinos in saline (100 μL; 6mg MO/kg) was injected in the tail vein of the corresponding mice.

***In situ* hybridization.** In situ hybridization was performed as previously described[3]. Briefly, mouse kidneys were fixed overnight in 4% PFA in PBS and processed directly for paraffin embedded. 12 μm sections were de-paraffinized and rehydrated, treated with proteinase K and fixed with 4% paraformaldehyde. Digoxigenin-labeled RNA probes were detected by alkaline-phosphatase-coupled anti-digoxigenin antibody (Roche Diagnostics, Mannheim, Germany) and NBT/BCIP was used as a chromogenic substrate to detect the digoxigenin-labeled probes (Boehringer, Mannheim, Germany). Sections were mounted in 50% glycerol in PBS and slices were photographed with a Leica DMR microscope under Nomarski optics.

Histological analysis. Kidney tissues were fixed in 4% PFA in PBS for 24 hours and embedded in paraffin. 3-μm sections were cut using a paraffin microtome with stainless steel knives. The sections were mounted on glass

slides, deparaffinized with xylene, dehydrated through graded series of ethanol, and stained with hematoxylin-eosin. To evaluate collagen deposition, sections were stained with Sirius Red (saturated aqueous solution of picric acid containing 0.1% Direct Red 80) (Sigma-Aldrich, St Louis, MO).

Immunohistochemical studies. Paraffin sections were deparaffinized and hydrated in graded ethanol series before staining with the peroxidase–antiperoxidase method. Antigens were retrieved by boiling for 20 min in 10mM citric acid solution (pH=6) or 10 mM Tris- 1 mM EDTA (pH=9). Endogenous peroxidase was blocked by incubation in 4% hydrogen peroxide. The sections were incubated overnight at 4ºC with the following primary antibodies: Biotinylated Lotus Tetragonolobus agglutinin, LTA (B-1325, Vector Laboratories, Burlingame, CA); Biotinylated Peanut agglutinin, PNA (B-1075, Vector Laboratories, Burlingame, CA); Tamm-Horsfall glycoprotein, THP (sc-20631; Santa Cruz Biotechnology, Santa Cruz, CA); alpha-smooth muscle actin, α-SMA (Sigma-Aldrich, St Louis, MO); Vimentin (sc-7557, Santa Cruz Biotechnology, Santa Cruz, CA); Phospho-NF-κB p65 (Ser276) (3037S, Cell Signaling Technology, Inc., Danvers, MA); Phospho-Smad2 (Ser465/467) (3101S, Cell Signaling Technology, Inc., Danvers, MA); F4/80 (MCA497GA, Serotec, Oxford,UK); Estrogen receptor alpha, ERα (sc-543, Santa Cruz Biotechnology, Santa Cruz, CA); Von Willebrand Factor, vWF (ab68545, Abcam, Cambridge, UK). The sections were incubated with the correspondent biotinylated secondary antibody, and sequentially incubated in ABC-Peroxidase Solution (Thermo Scientific, Rockford, IL) and 3,3'-Diaminobenzidine (DAB) (Sigma-Aldrich, St Louis, MO) was used as chromogen. Sections were lightly

counterstained with hematoxylin and were dehydrated and coverslipped. TUNEL staining was performed on sections using the In Situ Cell Death Detection Kit, (Roche Diagnostics GmbH, Mannhelm, Germany) according to the manufacturer's instructions.

X-Gal Staining. Kidneys were fixed in 4% paraformaldehyde in PBS for 2 hours on ice and stained for β-galactosidase activity by incubation in PBS containing 2 mM $MgCl_2$, 5 mM K4Fe(CN)6, 5 mM K3Fe(CN)6, and 0.4 mg/ml X-gal overnight at 37°C. After staining, the kidneys were washed in PBS and further fixed in 4% paraformaldehyde in PBS at 4°C. Kidneys were embedded in paraffin and 5 µm sections were cut, mounted and photographed with a Leica DMR microscope. In some experiments tissue sections were sequentially stained with antibodies or lectins as described above.

Quantitative RT-PCR (qRT-PCR). Total RNA was extracted using the Illustra RNAspin Mini RNA isolation kit (GE Healthcare, Little Chalfont, UK). 1µg of RNA was reverse transcribed using random hexamer primers according to the manufacturer's instructions (SuperScript II, Invitrogen). qRT-PCR was carried out on an ABI PRISM 7000 sequence detection system using the SYBR Green method (Applied Biosystems). RNA expression was calculated using the comparative Ct method normalized to Eif3. Data were expressed relative to a calibrator using the $2^{-(\Delta\Delta C_t)} \pm s$ formula.

Data analysis. Statistical analysis was performed using the GraphPad Prism software package. Results were expressed as mean ± SEM (standard error of

mean). Differences among different groups were tested by One-Way ANOVA or Two-Way ANOVA followed up by Tukey's test as appropriate. Differences between two groups were tested using Mann-Whitney test.

SUPPLEMENTARY REFERENCES

1. Rowe, R.G.*, et al.* Mesenchymal cells reactivate Snail1 expression to drive three-dimensional invasion programs. *The Journal of cell biology* **184**, 399-408 (2009).
2. Shao, X., Somlo, S. & Igarashi, P. Epithelial-specific Cre/lox recombination in the developing kidney and genitourinary tract. *Journal of the American Society of Nephrology : JASN* **13**, 1837-1846 (2002).
3. Boutet, A.*, et al.* Snail activation disrupts tissue homeostasis and induces fibrosis in the adult kidney. *The EMBO journal* **25**, 5603-5613 (2006).